

Figures

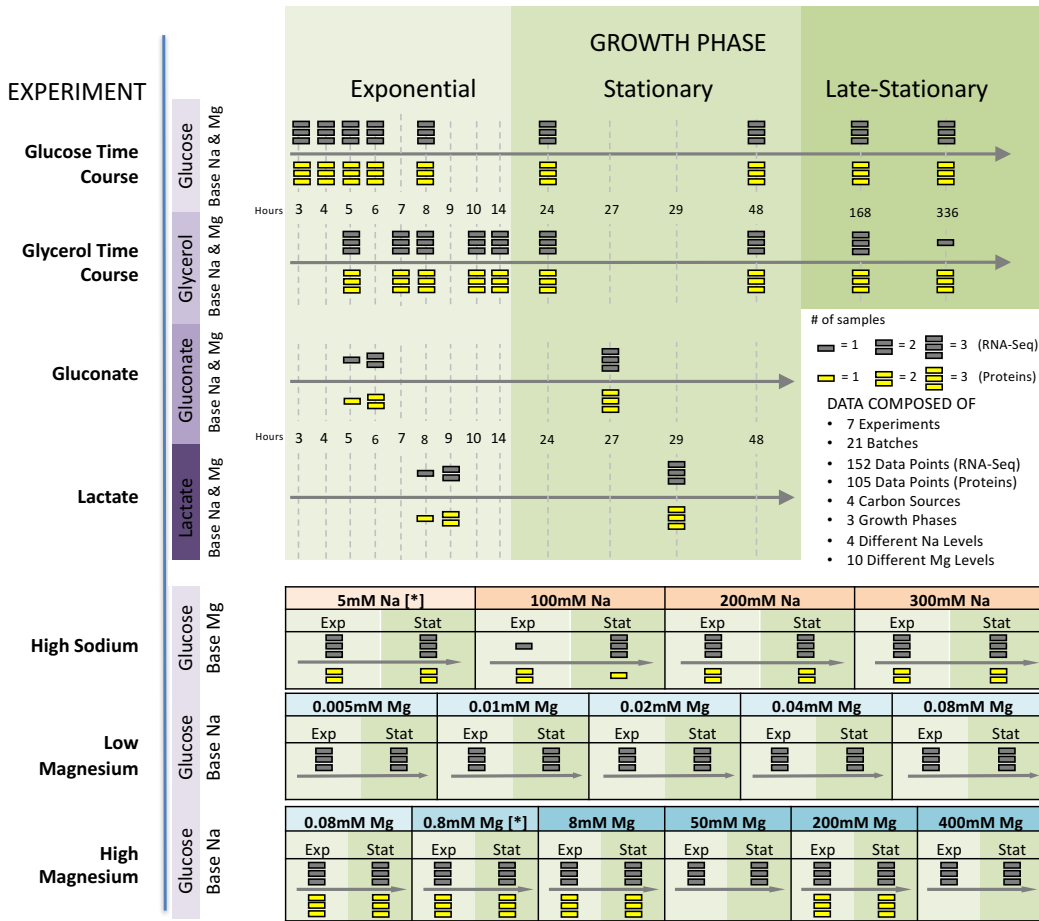


Figure 1: Experimental setup. We performed seven different experiments in which we varied the duration of growth and the temporal density of sampling, the carbon source, and ion concentrations. For each experimental condition, bacteria were grown in three biological replicates. We subsequently performed whole-transcriptome RNA-Seq for all experimental conditions and mass-spec proteomics for the majority of them. We considered four different carbon sources: glucose, glycerol, gluconate, and lactate; we also considered high sodium and both low and high magnesium levels. For the time-course and carbon-source experiments, we used base-level Na^+ (5 mM) and Mg^{2+} (0.8 mM) throughout (indicated by [*] in the sodium and magnesium experiments).

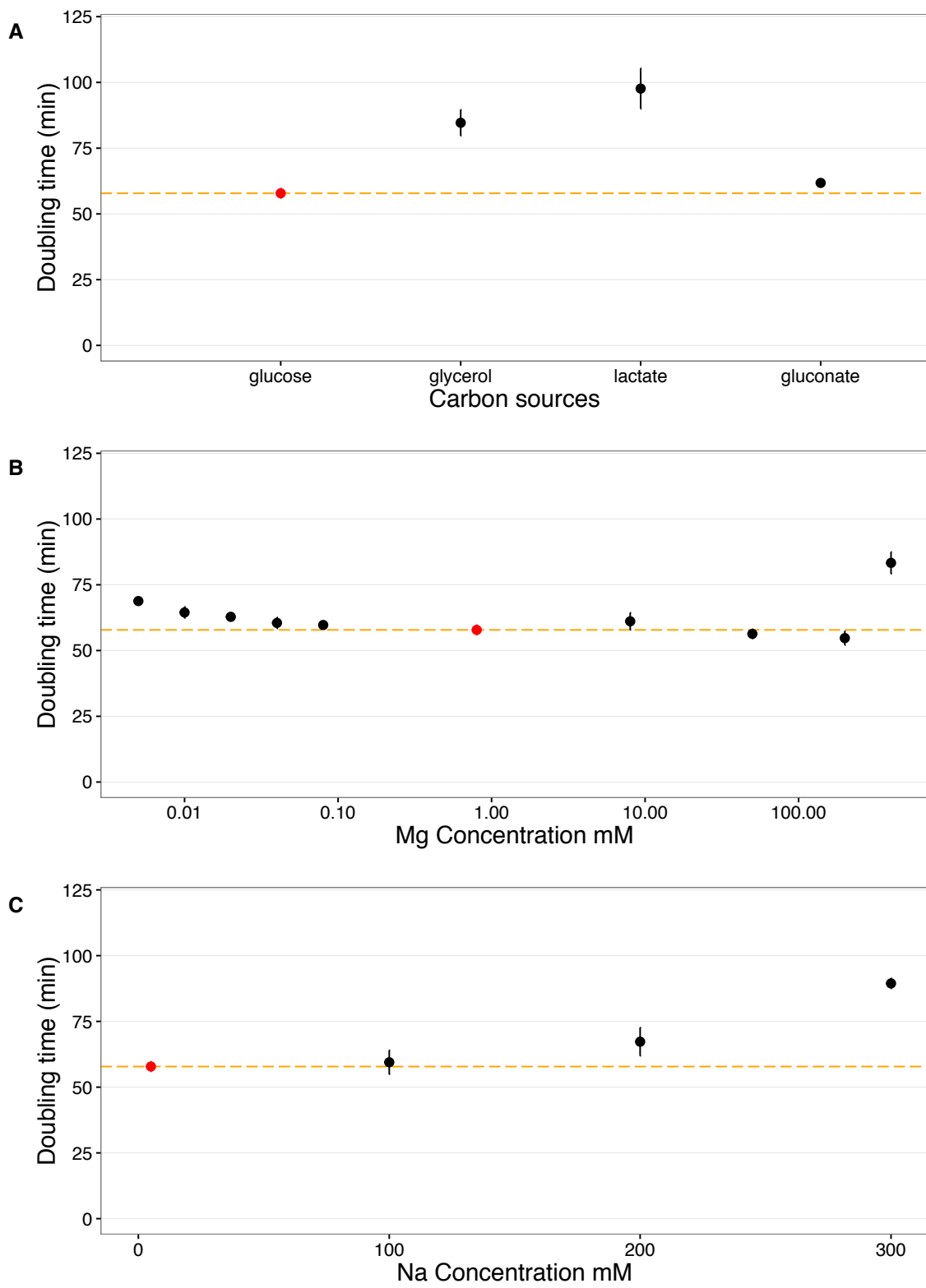


Figure 2: Doubling times under various growth conditions. We measured doubling times under exponential phase for all growth conditions. The red points and dashed orange lines represent the doubling time at the base condition (glucose, 5 mM Na⁺, 0.8 mM Mg²⁺). Doubling times were measured in triplicates and error bars represents 95% confidence intervals of the mean. (A) Doubling times with respect to carbon sources. (B) Doubling times with respect to Mg²⁺ concentrations. (C) Doubling times with respect to Na⁺ concentrations.

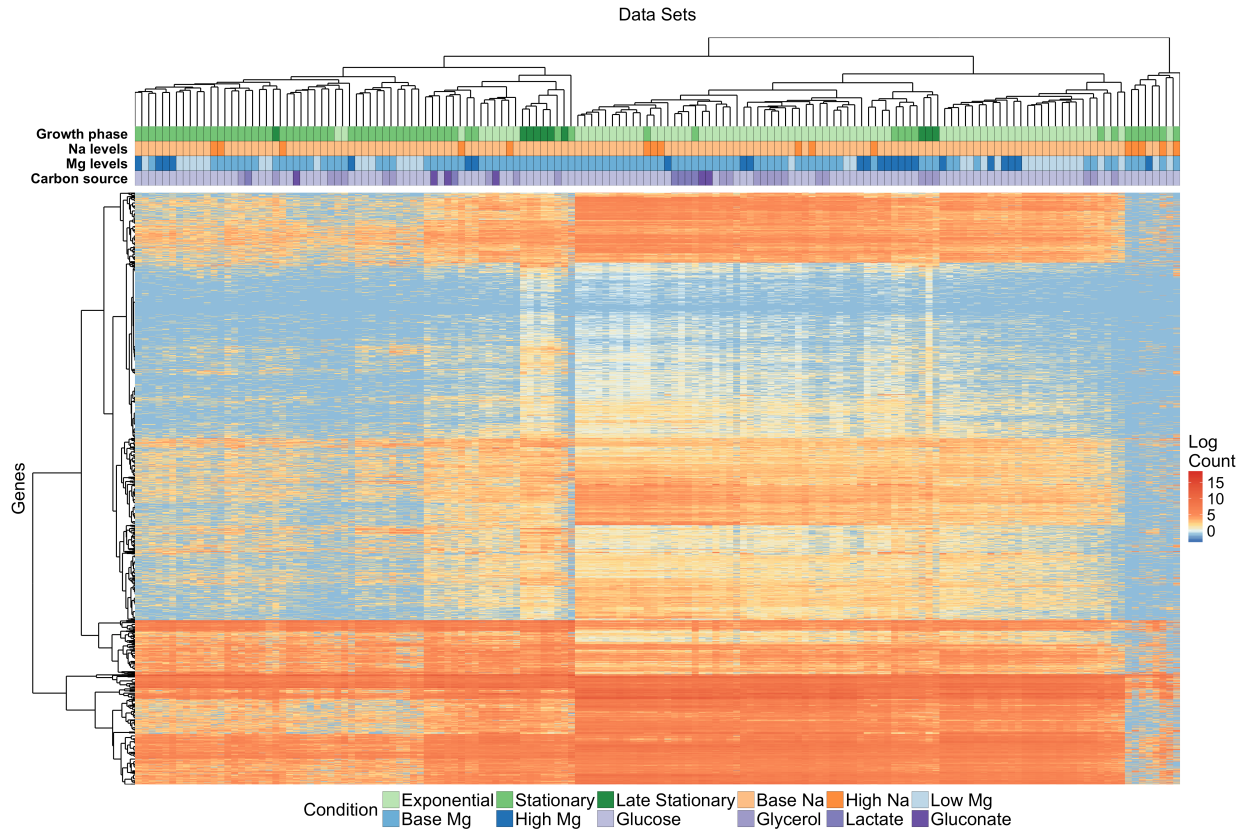


Figure 3: Clustering of mRNA abundances. The heatmap shows 4279 mRNA abundances for each of 143 samples, clustered both by similarity across genes and by similarity across samples. The growth conditions for each sample are indicated by the color coding along the top of the heatmap; the color coding is defined in the legend at the bottom.

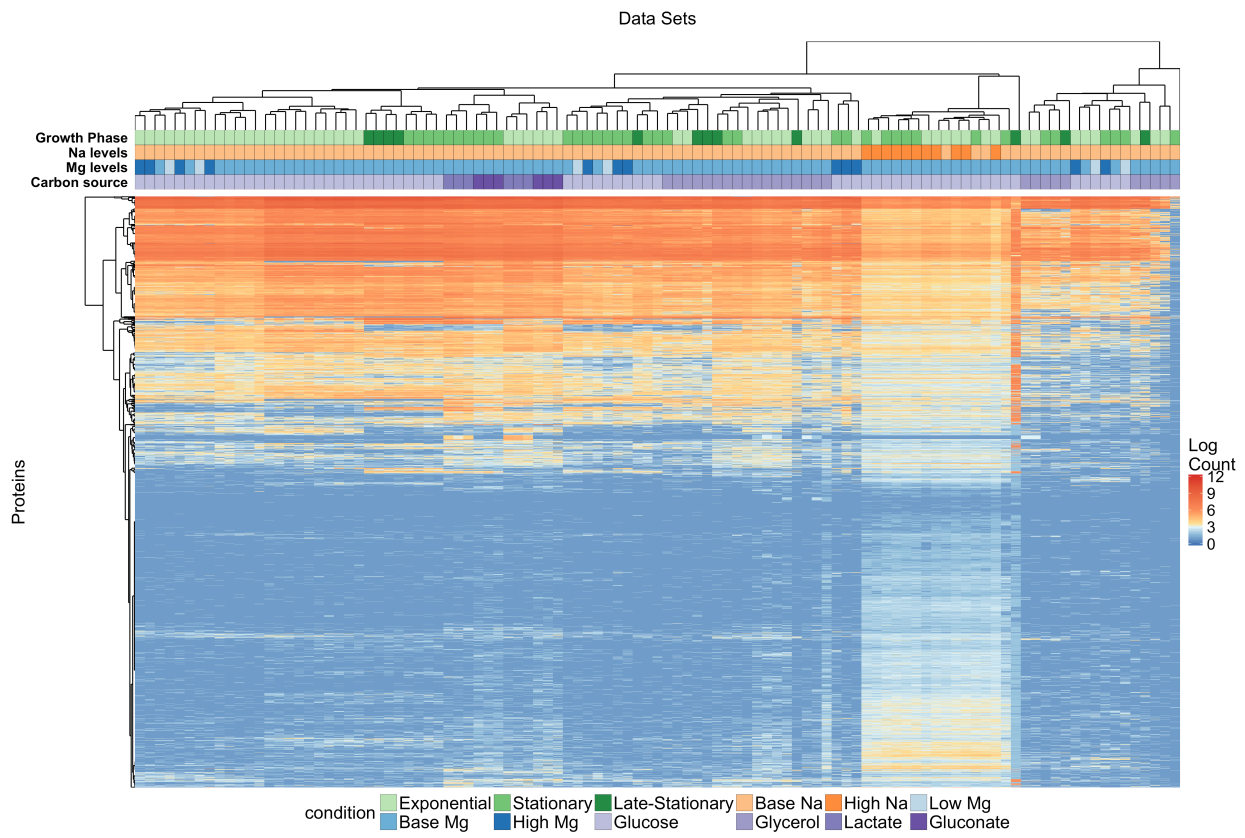


Figure 4: Clustering of protein abundances. The heatmap shows 4279 protein abundances for each of 101 samples, clustered both by similarity across genes and by similarity across samples. The growth conditions for each sample are indicated by the color coding along the top of the heatmap; the color coding is defined in the legend at the bottom.

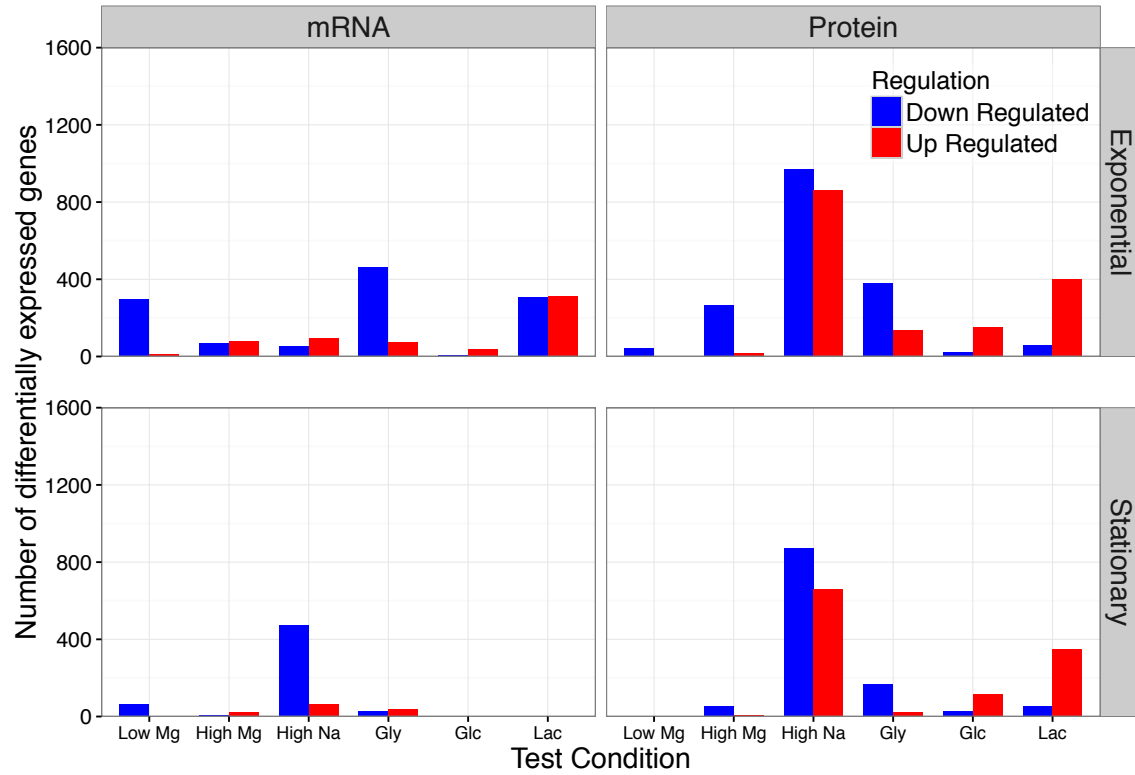


Figure 5. Number of differentially expressed genes under different conditions. We separately analyzed mRNA and protein abundances, each for both exponential and stationary growth phase. In all four cases, gene expression levels were compared to the corresponding condition with glucose as carbon source and baseline sodium and magnesium levels. Differentially expressed genes were defined as having at least a two-fold change relative to baseline and a false-discovery rate <0.05.

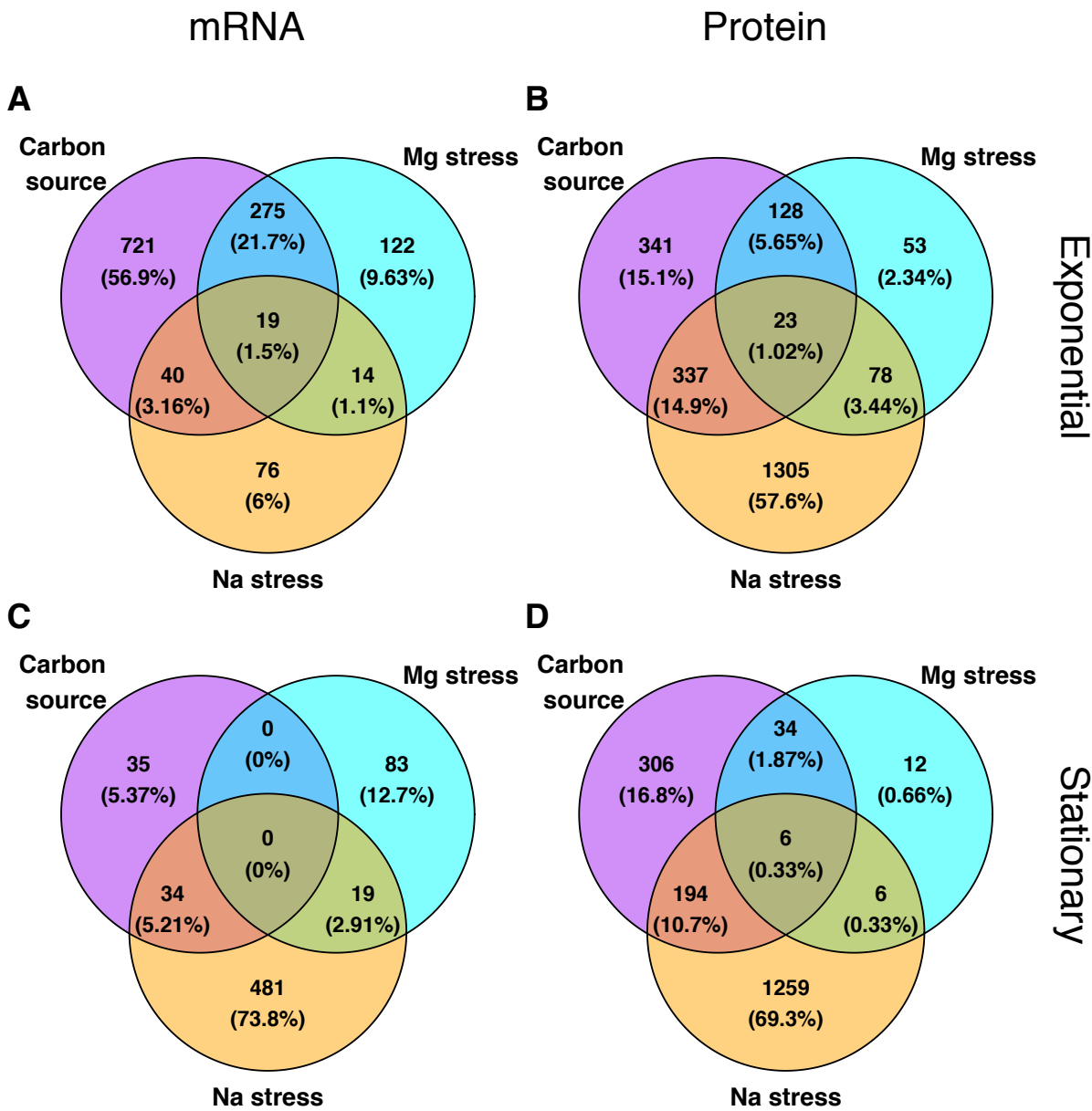


Figure 6: Overlap of differentially expressed genes among conditions. For all differentially expressed genes (identified as in Figure 5), we determined to what extent they were unique to specific conditions or appeared in multiple conditions. For simplicity, we here lumped all carbon-source experiments, all sodium experiments, and all magnesium experiments into one group each. Overall, we found relatively little overlap in the differentially expressed genes among these conditions. (A) mRNA, exponential phase. (B) protein, exponential phase. (C) mRNA, stationary phase. (D) protein, stationary phase.

A

mRNA	Protein	lowMg
1.Ribosome ▼▼▼ 2.Purine metabolism ▼▼▼		
1.Flagellar assembly ▼▼▼ 2.Sulfur metabolism ▲▲ 3.Nitrogen metabolism ▲▲	1.Biosynthesis of siderophore group nonribosomal peptides ▲▲ 2.Two-component system ▼▼▼ 3.Pyruvate metabolism ▼▼▼	highMg
1.Flagellar assembly ▼▼▼	1.Biosynthesis of amino acids ▼▼▼ 2.Biosynthesis of secondary metabolites ▼▼ 3.Biosynthesis of antibiotics ▼▼ 4.Metabolic pathways ▼▼ 5.Phenylalanine, tyrosine and tryptophan biosynthesis ▼▼▼	highNa
1.Ribosome ▼▼▼ 2.Biosynthesis of antibiotics ▼▼		glycerol
1.Pentose phosphate pathway ▲▲	1.Biosynthesis of siderophore group nonribosomal peptides ▼▼▼	gluconate
1.Pyruvate metabolism ▼ 2.Ribosome ▲▲	1.Citrate cycle (TCA cycle) ▲▲ 2.Pyruvate metabolism ▲▲ 3.Carbon metabolism ▲▲▲	lactate

B

mRNA	Protein	lowMg
1.Biosynthesis of siderophore group nonribosomal peptides ▲		highMg
1.Pyruvate metabolism ▼▼▼ 2.Pentose and glucuronate interconversions ▼▼ 3.Fructose and mannose metabolism ▼ 4.Glycolysis / Gluconeogenesis ▼▼	1.Biosynthesis of amino acids ▼▼▼ 2.Biosynthesis of secondary metabolites ▼▼ 3.Biosynthesis of antibiotics ▼▼ 4.Metabolic pathways ▼▼ 5.Phenylalanine, tyrosine and tryptophan biosynthesis ▼▼▼	highNa
	1.Biosynthesis of siderophore group nonribosomal peptides ▼▼▼	glycerol
	1.Biosynthesis of siderophore group nonribosomal peptides ▼▼▼	gluconate
	1.Citrate cycle (TCA cycle) ▲▲ 2.Biosynthesis of siderophore group nonribosomal peptides ▼▼▼ 3.Pyruvate metabolism ▲▲	lactate

Figure 7: Significantly differentially expressed KEGG pathways. For each condition, we show the top-5 differentially expressed KEGG pathways as determined by either mRNA or protein abundances. Empty boxes indicate that no differentially expressed pathways were found. The arrows next to pathway names indicate the proportion of up- and down-regulated genes among the significantly differentially expressed genes in this pathway. One up arrow indicates that 60% or more of the genes are up-regulated, two arrows correspond to 80% or more genes, and three arrows correspond to 95% or more genes being up-regulated. Similarly, down arrows indicate the proportion of down-regulated genes. (A) Exponential phase. (B) Stationary phase.

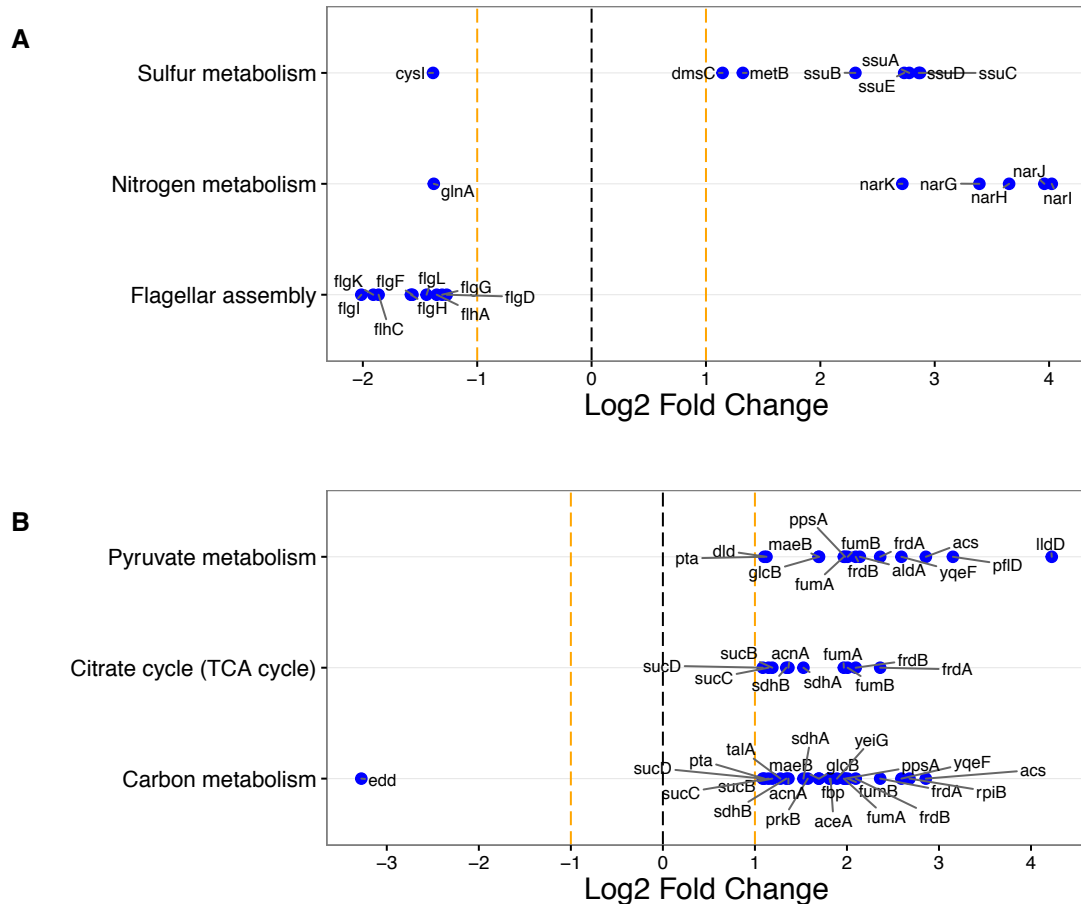


Figure 8: Examples of significantly differentially expressed KEGG pathways and associated genes. The top differentially expressed KEGG pathways are shown along the y axis, and the relative fold change of the corresponding genes is shown along the x axis. For each KEGG pathway, we show up to 10 of the most significantly changing genes. (A) Differentially expressed genes under high Mg^{2+} levels in exponential phase, as determined by mRNA abundances. (B) Differentially expressed genes under lactate as carbon source in exponential phase, as determined by protein abundances. Significant changes for all conditions are shown in Supplementary Figures 2–22.

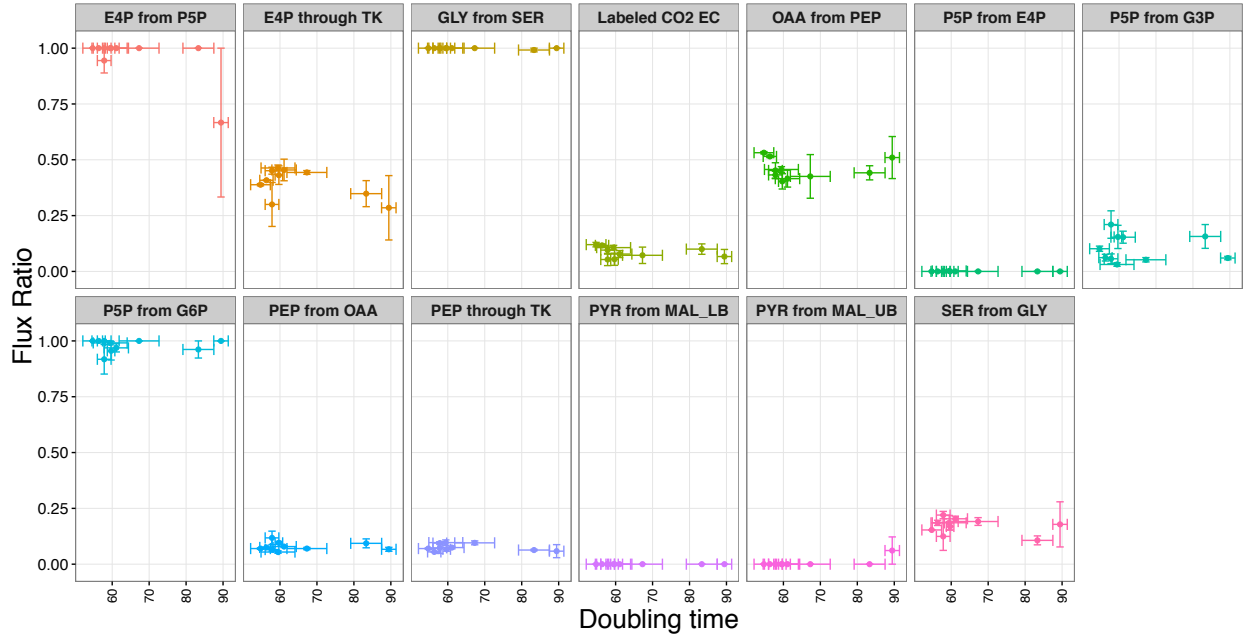


Figure 9: Flux ratios versus doubling times. 13 different flux ratios were measured for varying Na^+ and Mg^{2+} concentrations (Supplementary Figure 23). Here, these flux ratios are shown as a function of the corresponding doubling times. The specific fluxes considered and their shorthand labels as used here are defined in Ref. 31. There was no significant association between any of the flux ratios and doubling time after correction for multiple testing (Supplementary Table 6).

Tables

Table 1: Clustering of mRNA and protein abundances by different growth conditions. The z scores represent mean cophenetic distances between all pairs of conditions with the same label, normalized by the distribution of mean distances obtained after randomly reshuffling condition labels. The overall z score tests for significant clustering within a given variable, and the individual z score tests for significant clustering within a given condition. Significant clustering (defined as $|z|>2$) is indicated with a *.

mRNA

Variable	Overall z score	Condition	z score	# samples
Growth phase	-23.21 *	Exponential	-11.15 *	79
		Stationary	0.30	63
		Late stationary	-2.06 *	10
Carbon source	1.41	Glucose	1.53	115
		Glycerol	-1.51	25
		Lactate	-1.93	6
		Gluconate	-0.47	6
Mg Level	-1.82	Low Mg ²⁺	-0.75	36
		Base Mg ²⁺	-0.78	92
		High Mg ²⁺	-1.06	24
Na Level	-4.34 *	Base Na ⁺	-4.20 *	136
		High Na ⁺	2.85	16
Batch number	-2.11 *			

Protein

Variable	Overall z score	Condition	z score	# samples
Growth phase	-1.26	Exponential	-0.82	56
		Stationary	0.22	37
		Late stationary	-0.08	12
Carbon source	-2.80 *	Glucose	-2.34 *	66
		Glycerol	1.35	27
		Lactate	-2.73 *	6
		Gluconate	-2.63 *	6
Mg Level	-0.50	Low Mg ²⁺	0.85	6
		Base Mg ²⁺	-0.44	87
		High Mg ²⁺	-0.42	12
Na Level	-1.74	Base Na ⁺	-0.94	94
		High Na ⁺	-5.61 *	11
Batch number	-20.54 *			